3D fault imaging using windowed Radon transforms: an example from the North Sea

Geoffrey A. Dorn[1]* presents a flexible, novel and accurate approach to fault imaging using windowed Radon transforms applied to the F3 volume from the Southern North Sea.

Introduction

The interpretation of fault surfaces is key to understanding the subsurface geology represented in 3D seismic volumes. The geologic structure represented by seismic reflections can be auto-tracked in the volume. Faults, however, are imaged as discontinuities or changes in curvature in the seismic data. For many years, fault interpretation involved manually picking fault cuts on orthogonal slices through the seismic volume. These fault cuts were grouped into conceptual faults, and 3D fault surfaces were created from the fault cuts.

In the 1990s, the development of attributes to highlight discontinuities in 3D seismic data was pervasive in the industry. Perhaps the most well known of these efforts was the development of Coherence (Bahorich and Farmer, 1995; Gersztenkorn and Marfurt, 1996; Marfurt, et al., 1999). Although coherence or edge attributes highlighted faults in the seismic volume, the fault imaging was insufficient to support automatic extraction of the fault surfaces. These attributes provided guidance to the manual interpretation of faults in the 3D volumes.

This paper describes a portion of the history behind the development of techniques to improve 3D fault imaging to the point where fault surfaces can be automatically extracted from seismic volumes. A windowed Radon transform-based technique is then described and applied to the F3 survey from the North Sea. This technique produces fault images that are of sufficient quality to support automatic extraction.

Previous work on post-stack fault imaging

Since the late 1990s, there have been numerous efforts to further improve the imaging of faults in seismic volumes. Some techniques have used algorithms to improve on the imaging of faults provided by edge attributes (e.g., coherence, semblance or curvature data) while other approaches have used different attributes to highlight the faults in seismic volumes.

The first example of a process to improve on the fault imaging available in coherence volumes was proposed by Crawford and Medwedeff (1999). The first operator was designed to enhance lineaments on the horizontal slices. The second operator was designed to enhance lineaments on vertical slices resulting in what they called a Fault Enhance attribute volume. A third process was used to extract the prominent horizontal and vertical lineaments and linked them together to form fault surfaces.

AlBinHassan and Marfurt (2003) proposed using a Hough transform to detect faults in coherence and curvature volumes. Jacquemin and Mallet (2005) took this approach one step further by suggesting the use of a double Hough transform to detect and automatically extract faults. Randen et al. (2003) proposed tracking faults in coherence and other edge and curvature volumes using a model based on the behaviour of ants seeking and leaving a pheromone track along the shortest paths between nests and food sources.

Kadlec et al. (2008) proposed the use of level sets or evolving surfaces to improve imaging and tracking of faults in coherence

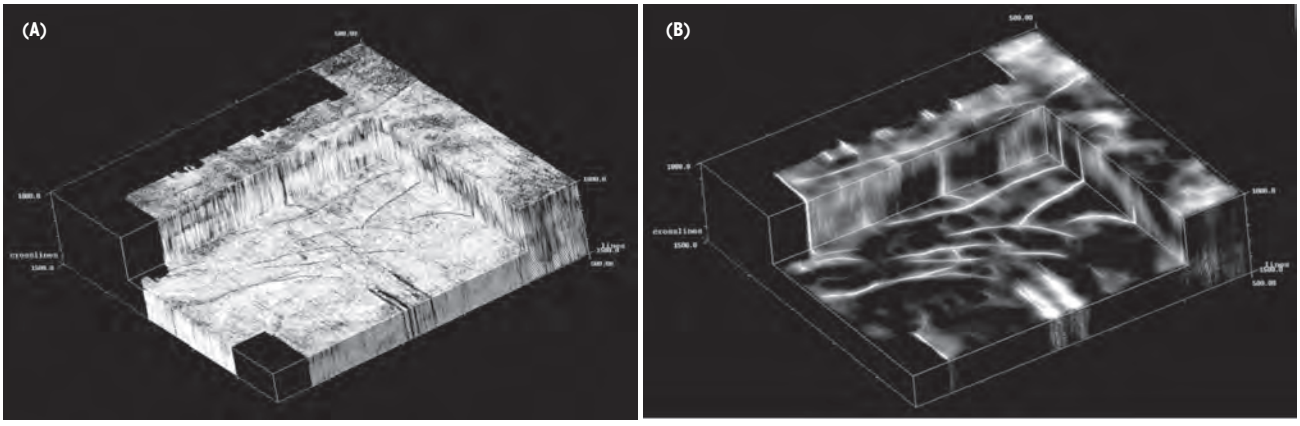

Figure 1 A coherence or edge attribute volume (a), and a fault enhanced volume (b) created by using the image enhancement algorithm described by Crawford and Medwedeff (1999).

[1] CGG
* Corresponding author, E-mail: geoffrey.dorn@cgg.com

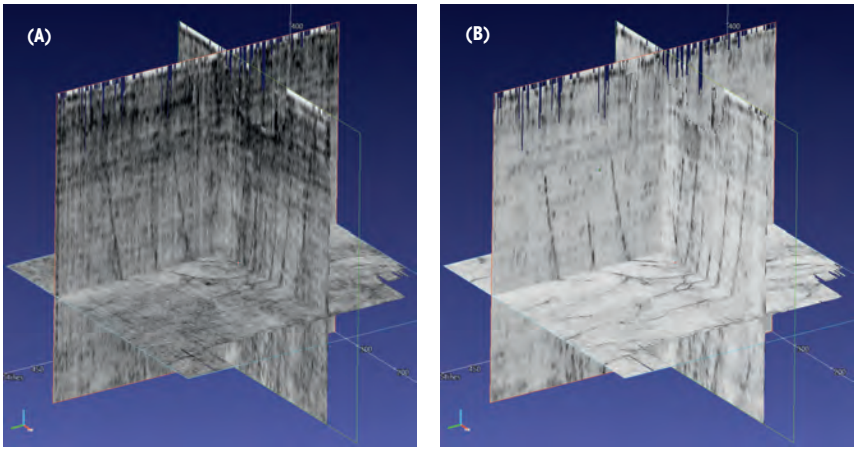

Figure 2 Slices from an edge attribute volume created (a) before and (b) after coherent and random noise have been filtered using structurally oriented post-stack filtering processes.

and fault enhanced volumes. More recently, Hale (2013) used a relatively small 3D operator to scan for dipping planar features in semblance volumes to find positions and orientations of highest likelihood of there being a fault in the 3D seismic volume.

Imaging 3D fault surfaces from edge attributes

In 1999, Crawford and Medwedeff (1999) patented the concept of applying processes to coherence volumes to improve the signal-to-noise ratio and continuity of fault imaging. The goal was to produce a 'Fault Enhanced' (FE) volume that would enable reliable automatic 3D fault surface extraction.

Their approach included a post-stack coherent noise filtering process to remove inline- and crossline-oriented footprint from the seismic volume. After footprint removal, they created a coherence volume, and applied image processing techniques to the coherence volume to produce an FE volume. This improved the signal-to-noise ratio and the continuity of the faults compared to the input coherence volume. Fault cuts were then extracted from horizontal and vertical slices of the FE volume, and then linked into fault surfaces.

Examples of the coherence and FE volumes are shown in Figure 1. Discontinuities associated with faults in the coherence volume are visible as black lineaments in the edge attribute volume in Figure 1a. The results of applying Crawford and Medwedeff's early fault enhance process are shown in Figure 1b. The resulting FE data shows the FE in a grey scale from black (low fault probability) to white (high fault probability).

From 2003 through 2016, further advances and improvements in this approach to imaging and extraction of fault surfaces were developed in the Geoscience Interpretation Visualization Consortium (GIVC)[1].

The consortium operated under the direction of this author from 2003 to 2015 at the BP Center for Visualization at the University of Colorado at Boulder, TerraSpark Geosciences, and then CGG.

Papers describing the application of this FE process to various 3D surveys from the Gulf of Mexico and the North Sea include Dorn and James (2005) and Dorn et al. (2007). First-generation FE and subsequent generations of AFE have been available in commercial software since 2006.

An AFE approach based on windowed Radon transforms

The initial work by Crawford and Medwedeff demonstrated the potential of fault extraction by improving the edge attribute imaging of faults. However, extensive testing from 2004 to 2008 identified several limitations of the original FE process:

- The process was very sensitive to noise in the seismic volume.
- Boundary conditions at the edges of the volume were poorly handled.
- Fault imaging was biased toward steep dips:
  - Low angle faults were imaged too deep and with too steep a dip.
  - Fault imaging was often inadequate for automatic fault extraction.
  - Faults were not imaged to their full extent.

In order to address these problems, a new workflow for fault enhancement was developed. The coherent noise filtering process (structurally oriented footprint removal) was re-engineered to handle any orientation of footprint (inline, crossline or oblique) and was structurally oriented. The manner in which the boundary conditions were handled was re-engineered to eliminate those problems at the edges of the seismic volume. Finally, a new AFE process, based on windowed Radon transforms was developed. The Radon transform-based AFE process images faults in the correct location and orientation regardless of fault dip, and images faults to their full extent. The quality of the fault imaging enables automatic fault surface extraction using a variety of techniques.

An initial version of this improved AFE was commercially available in 2009 and the process has been continually improved over the past 10 years in commercial software.

Noise filtering

An edge or coherence attribute amplifies the effect of any coherent or random noise that is present in the seismic volume.

[1] The GIVC Consortium member companies included Anadarko, Apache, BHP Billiton, BP, Chevron, ConocoPhillips, ExxonMobil, Magic Earth, Paradigm Geophysical, Shell, Stone Energy, and Repsol.

Before calculating an edge attribute, any remnant coherent and random noise remaining in the volume should be filtered out. A structurally oriented footprint removal process is applied to remove coherent noise from the volume (Dorn, 2018). A final structurally oriented random noise filter is then used to remove any remaining random noise.

Figure 2 illustrates the importance of applying structurally-oriented footprint removal and structurally-oriented random noise filtering to a seismic volume prior to calculating an edge attribute. Figure 2a shows an inline, crossline, and time slice of the edge attribute (horizon edge stacking or HES) calculated on a seismic volume from the US continental shelf in the Gulf of Mexico, offshore Louisiana, prior to applying structurally oriented noise filtering. Figure 2b shows the same slices where HES was calculated after footprint and random noise have been filtered from the volume. In this instance 19 footprint (wavelength, orientation) pairs were identified and filtered out of the seismic volume using the structurally oriented footprint removal process (Dorn, 2018). The improvement in the signal-to-noise ratio in the edge attribute is obvious as the faults are much more clearly imaged in Figure 2b.

The HES attribute used in this study is a structurally oriented edge attribute highlighting discontinuities in the seismic volume. Each plane in the operator is independently structurally oriented to the seismic dip at that level in the operator. The length of the operator may vary depending on whether the goal is to image faults, stratigraphic edges, or very small throw faults and fractures. Once coherent and random noise has been removed from the seismic volume, the edge attribute process is applied to the filtered seismic volume. The resulting volume is used as the input for the AFE fault imaging process used in this study.

Fault imaging

An improved AFE algorithm was developed based on the use of windowed Radon transforms (Dorn and Kadlec, 2011; Dorn et al., 2012). Conceptually, the problem of imaging faults using windowed Radon transforms is decomposed into three steps based on:

- The orientation in which faults are best imaged in edge attribute volumes (horizontal),
- The geologic concept that a fault is locally a dipping planar surface, and
- Using fault strike and dip to orient the AFE processes.

In the following discussion it is assumed that the scaling and polarity of the edge attribute volume is such that data ranges from 0 to 1, and that 0 = continuous (no edge) and 1 = discontinuous (a strong edge).

Edge attributes, such as HES, typically provide the best initial image of faults on horizontal (time/depth) slices. A windowed Radon transform, oriented horizontally and applied at each point in the edge attribute volume, yields a strike enhance (SE) output volume, and a strike (S) volume. The SE value at a point in the volume represents the probability that a horizontal lineament is passing through that sample. The S (strike orientation) value represents the strike of that lineament.

With a strike orientation (S) value at each sample in the volume, the second Radon transform is applied on vertical slices of the (SE) volume, where each vertical slice is oriented perpendicular to strike orientation defined by the S value at that sample (i.e., the vertical section is oriented in the azimuthal direction of local fault dip). A windowed Radon transform is applied on the vertical slice oriented perpendicular to strike at each sample in the (SE) volume. This produces a volume of dip enhance (DE) values, and a volume of Dip (D) values, which represent 2D vector dip in a direction that is perpendicular to strike in the S volume.

With the DE, S and D volumes, there is now sufficient information to orient a small planar surface to estimate fault dip at each sample in the DE volume – the geologic assumption of local planarity for a fault. The final step in the process integrates the DE values on dipping circular planes centered on each sample in the volume. This step also refines the estimate of the 3D dip vector at each point in the volume. The output from this final stage of the process is the FE value representing the probability that there is a dipping planar feature passing through each sample, and a final fault orientation (FO) value which is comprised of the (x,y,z) components of the 3D fault dip vector at each sample in the volume.

AFE can be defined by the following equations:

Strike Enhance:

At each sample point in the edge attribute volume, on a horizontal slice:

$$SE(x,y,z) = \max_{\sigma=0,180}\left[\int_{-a}^{a}\left(ES(\sigma,r)/2a\right)dr\right]$$

$$S = \sigma_{max}$$

Dip Enhance:

At each sample point in the SE volume, on the vertical slice oriented perpendicular to strike (S):

$$DE(x,y,z) = \max_{\delta=0,90}\left[\int_{-b}^{b}\left(SE(\delta,r)/2b\right)dr\right]$$

$$D = \delta_{max}$$

Fault Enhance:

At each sample point in the DE volume, on the dipping plane defined by

strike (S) and dip (D):

$$FE(x,y,z) = \int_{0}^{180}\int_{-c}^{c}(DE(\phi,c,r)/2c)\,dr\,d\phi$$

$$FO = (\phi_x,\phi_y,\phi_z)$$

where:

- ES = Edge attribute value at a point in the volume
- SE = Strike enhance attribute value at each point in the volume
- S = Strike of the ES discontinuity
- DE = Dip enhance attribute value at each point in the volume

- D = Dip of the SE discontinuity
- FE = Fault enhance (3D Fault probability scaled between 0 and 1) at each point in the volume
- FO = Fault orientation (x, y, and z components of 3D vector dip) at each point in the volume.
- (x,y,z) = The co-ordinates of the sample in the volume where the calculation is being applied.
- σ = Strike on the horizontal plane (time or depth slice) relative to North
- δ = Dip on the vertical plane oriented perpendicular to strike.
- ϕ = 3D dip vector
- a = Radius (r) in samples of the windowed Radon transform operator on a horizontal slice.
- b = Radius (r) in samples of the windowed Radon transform operator on a vertical slice oriented perpendicular to Strike (S).
- c = Radius (r) of the operator on the dipping plane defined by strike S and dip D.

The SE step improves the imaging of faults in the volume, particularly on horizontal slices (Figure 3a and b).

The DE step (Figure 4a) improves the imaging of faults in the volume, particularly in the vertical slices oriented perpendicular to strike in the volume. The FE step (Figure 4b) further improves the imaging of the faults and eliminates anything that is not a planar feature.

Each of the processes in the workflow improves the imaging of the faults while eliminating more of the background noise. Comparing figures 2a and 2b, the structurally oriented footprint removal and structurally oriented random noise filter processes substantially reduce the overall noise level in the edge attribute volume, while preserving the imaging of the faults. Comparing Figures 3a and 3b, the edge attribute volume calculated after filtering noise in the seismic data (Figure 3a) with the results of the strike enhance process (Figure 3b) shows another dramatic reduction in noise and a significant improvement in the continuity of the imaged faults.

Similarly, there are further reductions in noise and improved fault imaging in the DE results (Figure 4a) and in the FE results (Figure 4b). At the end of the workflow, the fault imaging is very sharp and the fault surfaces may readily be extracted in a number of ways.

Application to the F3 volume from the North Sea

The F3 Block data is from the southern North Sea, offshore Netherlands. The F3 survey was acquired in the late 1980s. The survey consists of 650 inlines, 950 crosslines with 25 x 25 m bins, and ranges from 0 to 1848 ms (4 ms sample rate). The original volume likely extended to 4 s in time, but was truncated approximately at the Top Rotliegende/Base Zechstein interface (1848 ms) prior to making the survey publicly available. Data was acquired using streamers: it is not wide-azimuth, and the offsets are shorter than for more modern surveys. The data was post-stack time-migrated. Substantial footprint remains in the processed volume.

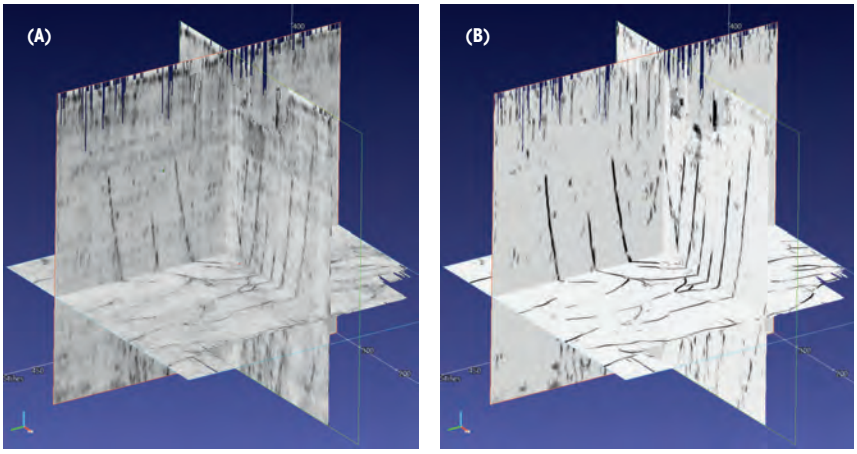

Figure 3 Slices (a) from an edge attribute volume after applying structure-oriented footprint removal, and (b) after the strike enhance step in AFE has been applied to that edge volume.

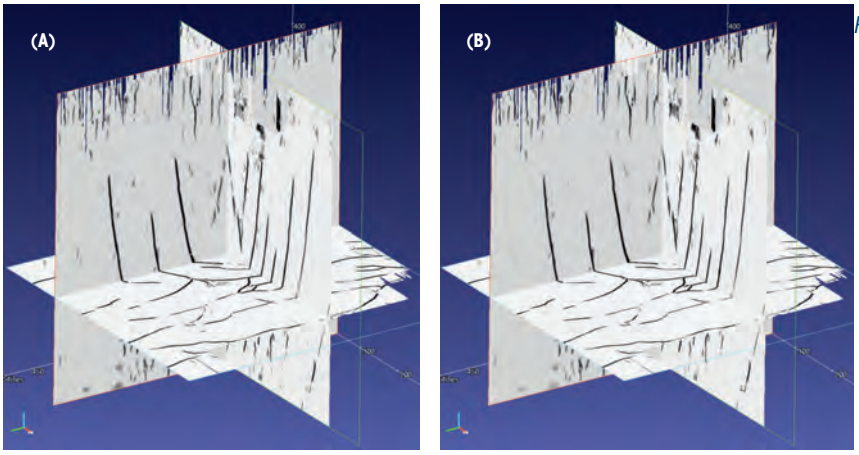

F3

Figure 4 Slices from the volume (a) after the dip enhance step in AFE has been applied, and (b) after the fault enhance step has been applied to the volume.

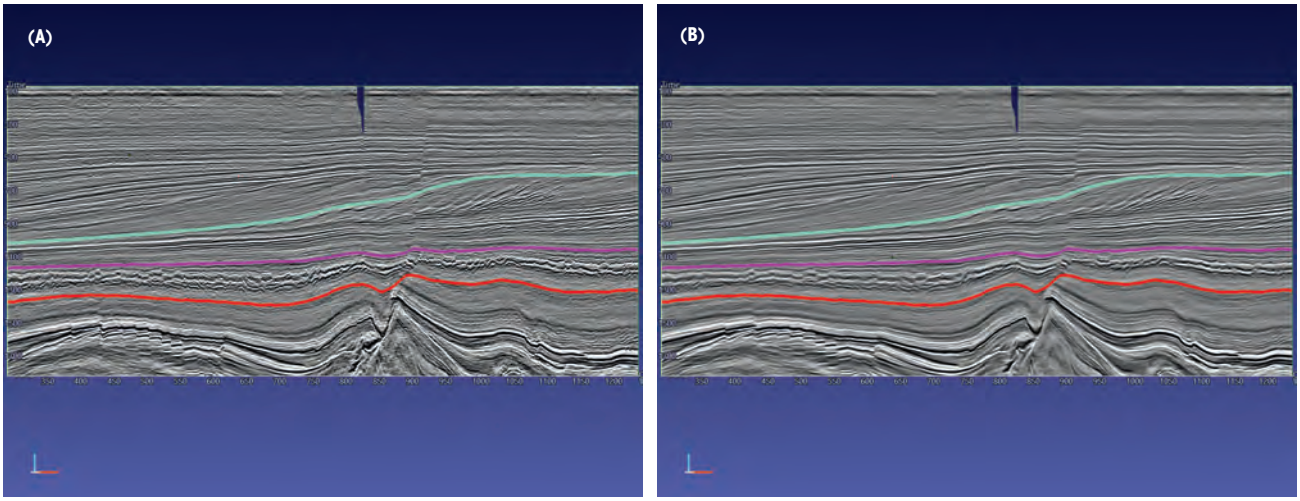

Figure 5 A portion of inline 306 from the F3 survey (a) before and (b) after structurally oriented footprint removal and random noise filtering.

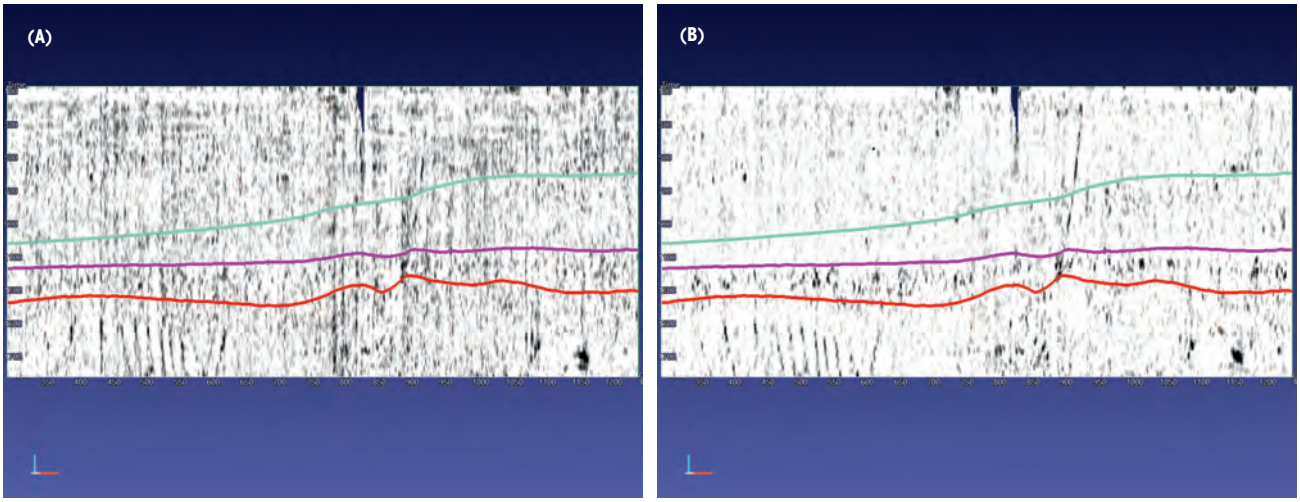

Figure 6 A portion of line 306 from the Horizon Edge Stack volumes calculated (a) before noise filtering, and (b) after noise filtering.

Volume noise filtering

In preparing the F3 volume for fault imaging, the 21 different footprint (orientation, wavelength) pairs that were identified in Dorn (2018) were removed from the volume using structurally oriented footprint removal. After coherent noise filtering, a 3x3 structurally oriented median filter was applied to the F3 volume to remove remaining random noise.

Figure 5 shows inline 306 from the F3 survey before (Figure 5a) and after (Figure 5b) the structurally oriented footprint removal and random noise filtering. Comparing the pre- and post-filtering versions of line 306, the reduction in noise level is quite clear. For detailed discussion of this noise filtering, see Dorn (2018).

For the purposes of the following discussion regarding the AFE results on the F3 volume, the volume as shown in Figure 5 has been split into four regions characterized by different types and degrees of faulting. Starting at the top:

- Region 1: Contains a few steeply dipping throughgoing faults
- Region 2: Numerous somewhat shallower dipping faults possibly associated with slope failure in the upper prograding system in the interval
- Region 3: Typical de-watered shale interval pervasive in the North Sea; shallower dip, and complex 'conical' faults.
- Region 4: Below the shale, extending into the Rotliegend are relatively steeply dipping normal faults

F3 volume horizon edge stack results

The application of structurally oriented footprint removal and random noise filtering had a substantial impact on the quality of the edge attribute. On line 306, Figure 6 shows a comparison between the edge attribute calculated on the unfiltered data (Figure 6a) and the edge attribute calculated on the filtered data (Figure 6b).

As expected, the coherent and random noise filtering has substantially reduced the background noise levels in the volume. In the lower left corner of the two images, the footprint removal process has removed the noise but retained the imaging of the steeply dipping faults in the Rotliegend (Region 4). One large throughgoing fault is substantially more apparent after noise filtering, extending from near the top of Region 4 to the surface in Region 1. The darker features in Region 3 are the beginning of fault imaging in the dewatered shale. Some of the darker features to the right of the throughgoing fault in Region 2 are also associated with faulting.

F3 volume AFE fault imaging

The HES volume (represented by the data shown in Figure 6b) is the input volume for the AFE workflow. Results of all three stages of AFE (strike enhance, dip enhance and fault enhance) are displayed in Figure 7.

The strike enhance process improves the imaging of the faults primarily on horizontal slices. Comparing Figure 6b with Figure 7a it is clear that the faults in all four regions are imaged with greater signal strength and continuity in the SE volume than they were in the edge volume. The DE step significantly improves the vertical continuity and definition of the fault surfaces (Figure 7b). Comparing the FE results (Figure 7c) with the edge volume (Figure 6b) the AFE process has significantly reduced noise in the volume while substantially improving the imaging and continuity of the faults.

If there is a need to further improve fault imaging while eliminating more noise from the volume, options include:

- Adjusting the AFE parameters to better image the faults (e.g., change the operator size, the dip window, etc. within AFE)
- Using the first-pass FE volume as the input 'edge attribute' volume for a second pass of AFE
- Using the FO (3D dip vector) volume to remove noise from the original edge attribute volume, and use this filtered edge volume as input for a second pass through AFE.

All three of these strategies usually produce refined fault imaging in the output volume. The results of the third approach to refinement of the fault imaging in F3 are examined here.

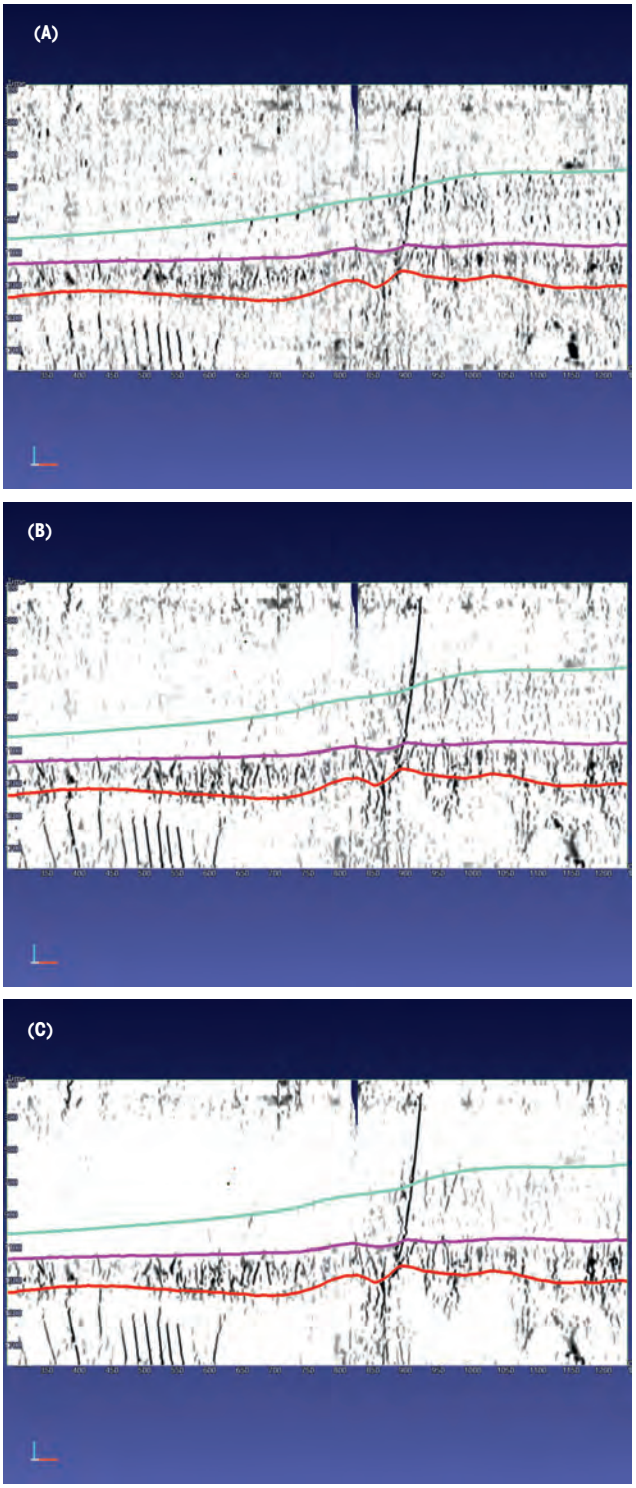

Figure 7 Inline 306 from the strike enhance step (a), the dip enhance step (b), and the fault enhance step (c).

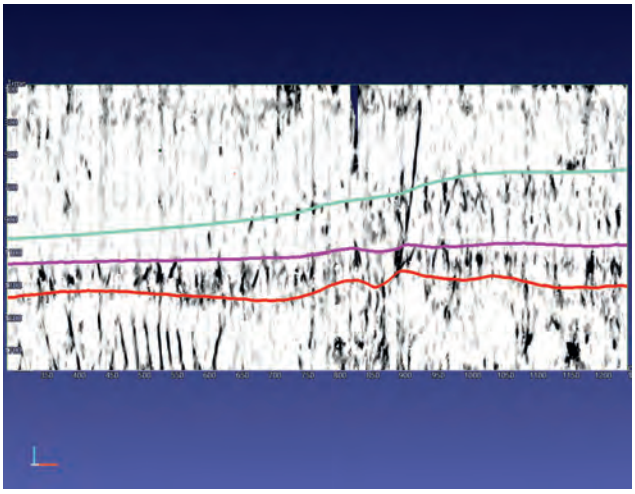

Figure 8 The result of applying fault structurally oriented random noise filtering to the edge attribute volume.

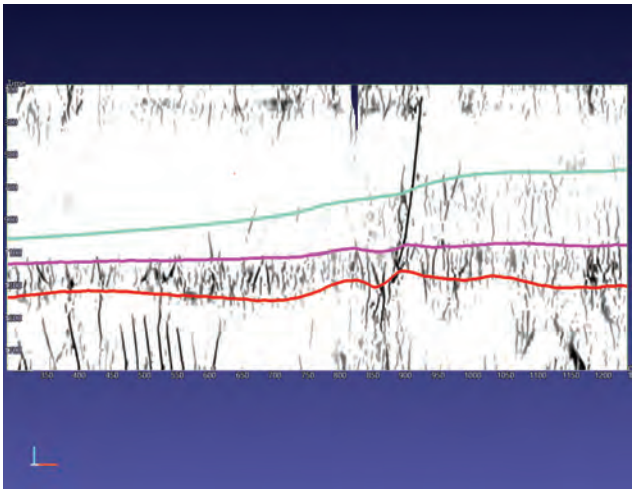

Figure 9 The FE volume produced by applying AFE to the filtered attribute volume shown in Figure 8.

The data in the FO volume represents the 3D vector dip for faults in the FE volume. Let the filter operator be a circular plane of a user-specified radius. If the operator is structurally oriented by fault dip, the planar filter operator will be oriented to fault dip when the centre point of the operator is on a fault in the FE volume. Otherwise, the operator will be oriented horizontally. With this design, any noise in the edge attribute volume will be attenuated while the image of faults will be improved. This is a unique example of structurally oriented filtering of the edge attribute data – where the random noise filter is oriented to fault dip rather than to horizon dip in the seismic volume.

Structural random noise filtering oriented by the FO volume was applied to the edge attribute volume shown in Figure 6b. The result, in Figure 8, shows a substantial reduction in the background noise level, and a substantial improvement in the imaging of faults throughout the volume.

The next step is to use this new filtered edge attribute volume as input for the AFE process. Figure 9 shows the results of running AFE on the structurally filtered edge volume in Figure 8.

Comparing the results in Figure 9 with those in the first run of AFE (Fig. 7c), the use of the edge attribute volume after fault structure oriented random noise filtering had two primary effects:

- The background noise level has been significantly reduced, and
- The fault imaging has been improved.

As a final step, Figure 10 shows seismic data from the F3 survey with the final fault results (the final FE volume) co-rendered in green with the seismic data. These images not only show that the faults are imaged, but they are imaged in the correct position with regard to the discontinuities in the seismic volume.

Conclusions

Interpretation of 3D fault surfaces in post-stack 3D seismic volumes has always been a key part of seismic structural interpretation. In the 1990s, a number of groups began working on attributes that they hoped would eventually lead to semi-automatic and automatic fault interpretation. In the mid-to-late 1990s, several attributes proved quite effective for imaging faults – including coherence, semblance and other discontinuity attributes, and curvature. Unfortunately, the fault imaging was not adequate to support automatic interpretation of fault surfaces.

Several years were spent experimenting with various approaches to improve edge attribute imaging of faults sufficiently to support automatic fault extraction. Based on the limitations of an initial approach, an advanced fault enhancement (AFE) process using modified windowed Radon transforms was developed. The process can accept any edge attribute, curvature attribute or combination of attributes that image faults as input. It generates both a fault-enhanced attribute and a fault orientation volume. The application of structurally oriented random noise filtering, based on fault orientation, to the edge attribute volume can substantially improve the fault imaging. Using the filtered edge attribute volume as input to AFE can substantially improve the quality of the imaged faults, and the ability to extract faults automatically.

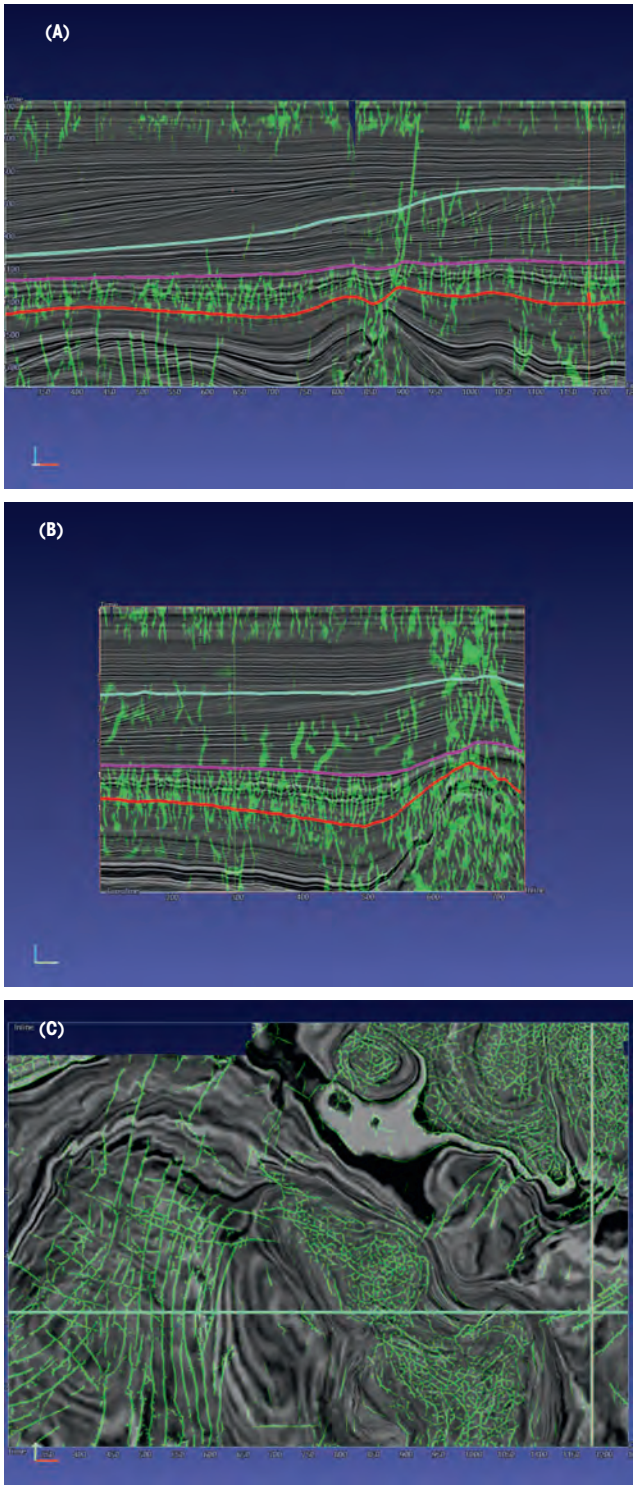

Figure 10 Slices from the noise-filtered seismic volume (Figure 5b) co-rendered with the final FE results obtained from the noise-filtered edge attribute volume (Figure 8). The co-rendering shows the accurate and precise imaging of the faults on inline (a), crossline (b), and time slice (c) views.

Acknowledgements

I would like to thank CGG for permission to publish this paper. I would also like to acknowledge the Open Seismic Repository (OSR) and its website maintained by dGB Earth Sciences from which the F3 data set can be downloaded. The technologies for enhanced fault imaging and extraction, and structurally oriented noise filtering described in this paper were developed at Ter-

raSpark Geosciences and CGG GeoSoftware by the author and several colleagues and have been in InsightEarth since 2009. All data processing, display and interpretation was performed using CGG GeoSoftware's InsightEarth advanced seismic interpretation software package.

References

AlBinHassan, N.M. and Marfurt, K.J. [2003]. Fault detection using Hough Transforms. *73rd Annual International SEG Meeting*, Expanded Abstracts, 1719-1721.

Bahorich, M.S. and Farmer, S.L. [1995]. 3-D seismic coherency for faults and stratigraphic features. *The Leading Edge*, **14**, 1053–1058.

Crawford, M. and Medwedeff, D. [1999]. *Automated extraction of fault surfaces from 3-D seismic prospecting data*. U.S. Patent No. 5,987,388.

Dorn, G.A. and James, H.E. [2005]. Automatic Fault Extraction in 3-D Seismic Interpretation. *67th EAGE Conference and Exhibition*, Expanded Abstracts, F035.

Dorn, G.A., James, H.E., Evins, L., Marbach, J. and Coady, F.A. [2007]. Applications of Automatic Fault Extraction (AFE) in a Variety of Geologic Environments: Results, Limitations, and Suggested Improvements. *AAPG Annual Convention and Exhibition*, Expanded Abstracts.

Dorn, G. and Kadlec, B. [2011]. Automatic fault extraction in hard and soft rock environments. *SEPM Society for Sedimentary Geology*, **31,** 12.

Dorn, G.A., Kadlec, B. and Murtha, P. [2012]. Imaging faults in 3D seismic volumes. *82nd Annual International SEG Meeting*, Expanded Abstracts.

Dorn, G.A. [2018]. Structurally oriented coherent noise filtering. *First Break*, **36** (5), 37-45.

Gersztenkorn, A. and Marfurt, K.J. [1996]. Eigenstructure based coherence computations. *66th Annual International SEG Meeting*, Expanded Abstracts, 328–331.

Hale, D. [2013]. Methods to compute fault images, extract fault surfaces, and estimate fault throws from 3D seismic images. *Geophysics*, **78** (2), 033–043.

Jacquemin, P. and Mallet, J.L. [2005]. Automatic fault extraction using double Hough transform. *75th Annual International SEG Meeting*, Expanded Abstracts, 755-758.

Kadlec, B., Dorn, G., Tufo, H. and Yuen, D. [2008]. Interactive 3D computation of fault surfaces using level sets. *Visual Geoscience*, **13**, 133-138.

Marfurt, K.J., Sudhakar, V., Gersztenkorn, A., Crawford, K.D. and Nissen, S.E. [1999]. Coherency calculations in the presence of structural dip. *Geophysics*, **64**, 104-111.

Randen, T, Pedersen, S.I., Sonneland, L. and Steen, O. [2003]. New paradigm of fault interpretation. *73rd Annual International SEG Meeting*, Expanded Abstracts, 350-353.